Molecular dynamics simulation of CO_2 dissolution-diffusion in multi-component crude oil

Yulong Kang[1], Lei Zhang[1], Juan Luo[2], Yuchuan Guo[2], Shiying Cheng[2], Di Wu[2], Kaifen Li[2] and Shiqiang Guo[2]*

[1]Research Institute of Yanchang Petroleum (Group) Co., Ltd., Xi'an, China, [2]State Key Laboratory of Petroleum Resources and Prospecting, China University of Petroleum (Beijing), Beijing, China

In order to study the dissolution-diffusion process and mechanism of CO_2 in multi-component crude oil, a model of multi-component crude oil system with octane as the main component and 16 other alkanes as a compound was constructed by using molecular dynamics simulation method. We estimated the CO_2 density distribution in crude oil model and the shift in crude oil model volume change. We then investigated the microscopic influence mechanism of CO_2 dissolution-diffusion on the volume expansion of crude oil by simulating the action of CO_2 dissolution-diffusion in the multi-component crude oil model. Based on the variation law of mean square displacement between crude oil molecules, the dissolution and diffusion coefficients of CO_2 were predicted, and the influence of CO_2 dissolution-diffusion on crude oil mobility was analyzed. It is found that temperature intensifies the molecular thermal motion and increases the voids between alkane molecules, which promotes the dissolution of CO_2 and encourages CO_2 molecules to transmit, making the crude oil expand and viscosity decrease, and improving the flow ability of crude oil; with the enhancement of given pressure, the potential energy difference between the inside and outside of the crude oil model becomes larger, and the voids between alkane molecules become larger, which is favorable to the dissolution of CO_2. Nevertheless, the action of CO_2 molecules' diffusing in the crude oil sample is significantly limited or even tends to zero, besides, the mobility of crude oil is affected due to the advance of external pressure. The mechanism of CO_2 dissolution and diffusion in multi-component crude oil is revealed at the microscopic level, and provides theoretical guidance for the development of CO_2 flooding.

KEYWORDS

CO_2, dissolution-diffusion, multi-component crude oil system, molecular dynamics simulation, mobility

1 Introduction

CCUS, the abbreviation for Carbon Capture Utilization and Storage technology, has been developed in recent years with the global attention to greenhouse gas emissions and other ecological issues. CCUS technology is not only effective in improving global warming, but also significant for achieving zero carbon emissions by 2050. According to the International Energy Agency, CCUS technology will achieve 38% of the emission reduction in the chemical and engineering industry and is expected to contribute about 14% of the CO_2 emission reduction by 2050 (Mi and Ma, 2019; Jin and Chen, 2020; Qin et al.,

2020; Zhang et al., 2022). CCUS technology can be further divided into oil and gas reservoir utilization (CCUS-EOR/EGR), chemical utilization, and biological utilization depending on the utilization method. CCUS-EOR technology is to inject the captured CO_2 into a reservoir in the development stage with complete geological structure and adequate basic information, to enhance the recovery of crude oil through CO_2 flooding and to achieve CO_2 burial (Ku et al., 2023). This technology is not only highly economically viable, but also has a wide range of applications and a very promising future.

Overseas CO_2 flooding originated in the 1950s (Whorton et al., 1952). In the 1980s, it was gradually applied in the oil field and began to be promoted commercially. Since 2000, the globe concern about environmental issues and the continuous development of engineering technology have further promoted the innovation of CO_2 flooding technology (Shen and Liao, 2009). Around the 1960s, China started to pay close attention to CO_2 flooding technology and conducted indoor flooding experiments, and carried out field tests in layer 4-7 of Pulin Daqing oilfield and in the eastern transition zone of Sanan; during the 1990s, Jiangsu Fumin oilfield carried out experiments on CO_2 huff and puff (Chen et al., 2011). Before entering the 21st century, due to the lack of understanding and experimental support for this technology, coupled with the lack of CO_2 gas sources in China and serious gas channeling in the oilfield experiments, the development of CO_2 flooding technology in China had been slow (Gao et al., 2014; Zhao et al., 2017; Li, 2018). Over past 10 years, the internal CO_2 flooding and storage field tests had made a remarkable progress which had three phases: pre-experiments, extended tests and industrial application, with increasingly abundant types of reservoirs and scales of tests, achieving certain results and accumulating some practical experience (Luo et al., 2013). Among all enhance oil recovery (EOR) technologies, the most well-known and effective way to enhance the oil production efficiency is to inject CO_2 into the reservoir, furthermore, the injected CO_2 can achieve the goal of CCUS energy saving and emission reduction (Yuan et al., 2020). The reasons in terms of mechanism why CO_2 flooding can enhance oil recovery is that the solution of CO_2 in the crude petroleum causes volume expansion of crude oil and increases oil saturation in the pore; in addition, CO_2 can diffuse easily inside oil and water, giving the opportunity that the CO_2 can redistribute and stabilize the balance of phase system, which acts an effective part in the relative permeability of oil and water (Hu et al., 2017; Guo et al., 2018; Jia et al., 2019; Li et al., 2019; Li, 2020; Jia et al., 2021).

To take into account the limitations of the complex dissolving and diffusing action of CO_2 inside oil and water, and the inability of indoor experiments to simulate the microscopic oil drive efficiency of CO_2, the author chose the molecular dynamics simulation method to carry out the research. Molecular dynamics simulation is a non-quantum mechanical method to work out problems at the molecular level based on the fundamental theory of classical Newtonian mechanics. The calculation process mainly relies on the position or average configuration of the nucleus to establish the required force field function to describe the molecular structure and energy, which is a more widely used calculation method, and it has certain advantages in analyzing the changes of microscopic properties such as intermolecular forces and molecular morphology. A crude oil system model which contains multiple

TABLE 1 Oil composition analysis data.

Component	Mole %	Plus fraction analysis	Mole %
C1	14.446		
C2	6.487	C1–C4	41.793
C3	12.674	C5+	58.207
C4	8.186		
C5	3.958		
C6	3.223	C1–C8	66.605
C7	4.893	C9+	33.395
C8	12.738		
C9	7.632		
C10	7.162	C1–C16	97.856
C11	3.577	C17	2.144
C12	3.109		
C13	2.969		
C14	2.527		
C15	2.368		
C16	1.907		
C17	2.144		
Total	100		

alkane components is constructed and the action of dissolution-diffusion of CO_2 in the multi-component crude oil model is simulated by applying the simulation method of molecular dynamics in this article. The CO_2 density distribution in crude oil as well as the volume change of crude oil are calculated, and the microscopic impact mechanism of CO_2 dissolution-diffusion on the volume expansion of crude oil is further analyzed. The dissolution and diffusion coefficients of CO_2 were predicted based on the variation law of mean square displacement between crude oil molecules, and the impact of CO_2 dissolution diffusion on crude oil mobility was analyzed. The mechanism of CO_2 dissolution-diffusion in multi-component crude oil is revealed at the microscopic level, and provides theoretical guidance for the development of CO_2 flooding.

2 Construction of the multi-component crude oil system model

Primarily based on the results of laboratory determination of the chemical compositions of crude oil, a model of crude oil was constructed within our paper, the crude oil model is mainly composed of octane, including 17 kinds of alkane components such as methane and ethane (Table 1), the density at 20°C of this model is 0.82 g/cm³. The Visualize module in Material Studio software was used to build a model of each alkane molecule in the crude oil component (as shown in Figure 1). In addition, a molecular model of CO_2 (shown in Figure 2) was constructed for
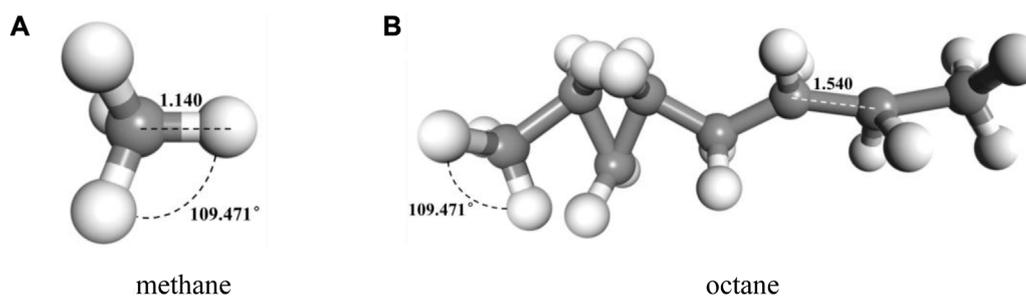
FIGURE 1
Typical molecular model of components of oil. **(A)** methane **(B)** octane.

FIGURE 2
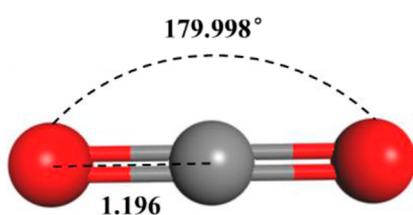CO_2 molecular model.

subsequent simulation of the CO_2 motion in the crude oil model (Jia et al., 2021).

In accordance with the established molecular models of alkanes and CO_2 above, the geometry and energy optimization of each molecular model were carried out and the optimized the molecular model structure was obtained by using the Forcite component, as shown in Figure 3. Figure 4 indicated that we used the Construction tool which is belong to the Amorphous Cell Tools component to build the multi-component crude oil molecular system model in accordance with the experimental testing consequences of crude oil components with the dimensions of $42.67 \times 42.67 \times 42.67$ Å^3 and the density of it is set to 0.82 g/cm^3 in accordance with the real crude oil density. To ensure that the properties of the system remain unchanged

during the simulation process, the crude oil system model is therefore subjected to three-dimensional periodic boundary conditions. CO_2 was added to the multi-component crude oil molecular system model, and the temperature were set to 313 K, 353 K, 393 K and the pressure were set to 10–50 MPa, in units of 10 MPa respectively in order to be similar to the reservoir properties. This part is a preparation for the research of the action of the CO_2 dissolution and diffusion in crude oil under different reservoir conditions. It should be noted that the idea of establishing the model is also applicable to other multi-component fluids including two phases of oil and gas or three phases of oil, gas and water, but it needs to be further determined according to experimental results and research objectives. Multi-component fluids are more reasonable in real formation fluid characterization and simulation.

3 Simulation method and validation

Author used the BIOVIA Material Studio 2019 software package for molecular dynamics simulations. First, the geometric and energy optimization of the multicomponent crude oil model was performed using steepest descent method to obtain the optimized structures for different temperature and pressure conditions. After that, the kinetic equilibrium was performed, and the force field parameters for both CO_2 and n-alkanes were assigned using the COMPASS force field developed by Sun et al. which is suitable for organic molecules and
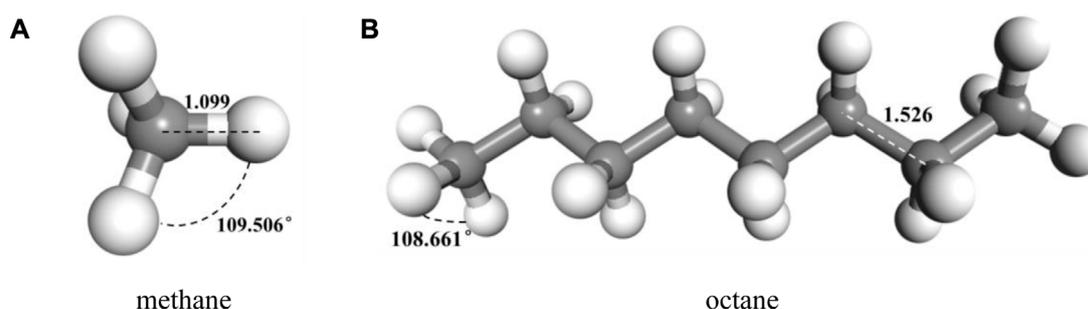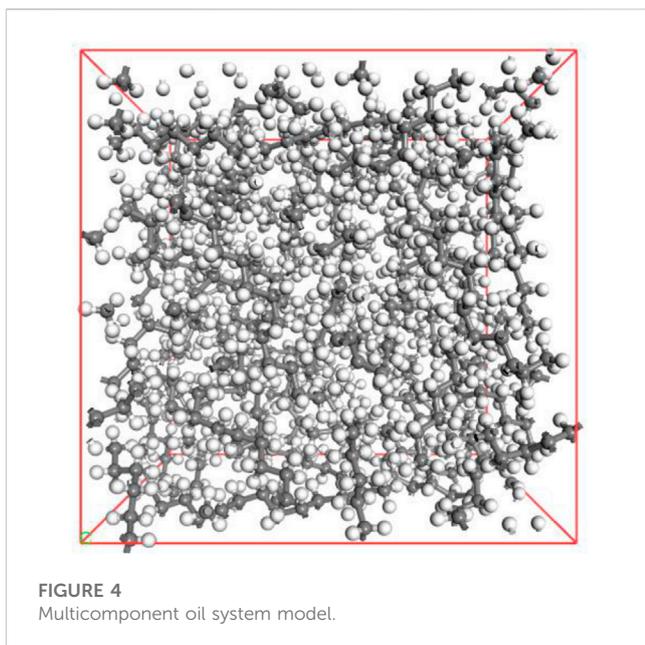

FIGURE 3
Typical molecular model of components of oil after geometric and energy optimization **(A)** methane **(B)** octane.

FIGURE 4
Multicomponent oil system model.

$$E = \sum_{i>j} \frac{q_i q_j}{r_{ij}} + \sum_{i>j} E_{ij} \left[2\left(\frac{r_{ij}^0}{r_{ij}}\right)^9 - 3\left(\frac{r_{ij}^0}{r_{ij}}\right)^6 \right] \qquad (2)$$

$$r_{ij}^0 = \left(\frac{(r_i^0)^6 + (r_j^0)^6}{2} \right)^{\frac{1}{6}} \qquad (3)$$

where ij denotes an atomic pair, E_{ij} is the potential well depth, r_{ij}^o is the zero potential distance of the atomic pair, and r is the distance between two atoms.

The other kinetic simulation parameters are: the canonical ensemble (NVT), temperature control using the Nosé-Hoover method, with the temperature set to 313, 353, and 393 K respectively; after that, the isothermal isobaric system synthesis (NPT) is selected, with the pressure set to 10–50 MPa, in units of 10 MPa, respectively, and the Berendsen method for pressure control. All other parameters were consistent in both equilibria, including: Ewald and Atom Based ways were adopted for electrostatic interaction as well as van der Waals interaction, separately. The dynamic simulation of 1 ns (1,000,000 steps) was performed with a step size of 1 fs at a distance of 1.25 nm. The consequences of the simulation procedure were exported every 1,000 steps which divided into two parts, the first part including 400 ps, they were applied to maintain the balance of the system, and the other part containing 600 ps was utilized for collecting the density data in whole system.

The way in which we calculate the crude oil molecular system density at a temperature of 20°C is to apply the simulation of molecular dynamics, afterwards, we compared it with the US NIST database, as shown in Figure 5. The difference between the value of crude oil system density as determined via molecular dynamics simulation that used in our article and the density value of reference given by NIST database is slight, which indicating that the established multi-component crude oil system model and procedure of simulation are reasonable.

inorganic covalent bond molecular systems, and its potential energy function form is expressed as:

$$E_{total} = E_{bond} + E_{angle} + E_{torsion} + E_{cross} + E_{vdw}$$
$$+ E_{coulombic} \qquad (1)$$

where the first previous four terms show the bonding energy and the last two terms denote the non-bonding interaction energy. The non-bonding interaction energy can be represented by the Lennard-Jones 9-6 potential and the Coulomb electrostatic potential. The Lennard-Jones 9-6 potential describes the potential energy due to the weak repulsive and gravitational forces of the van der Waals force. Its specific form is:

FIGURE 5
Comparison of octane density values in oil models under different temperature and pressure conditions.

FIGURE 6
Dissolution density distribution of CO_2 in oil system model under varying temperature and pressure conditions **(A)** 313 K-10 MPa **(B)** 313 K-50 MPa **(C)** 353 K-10 MPa **(D)** 353 K-50 MPa **(E)** 393 K-10 MPa **(F)** 393 K-50 MPa.
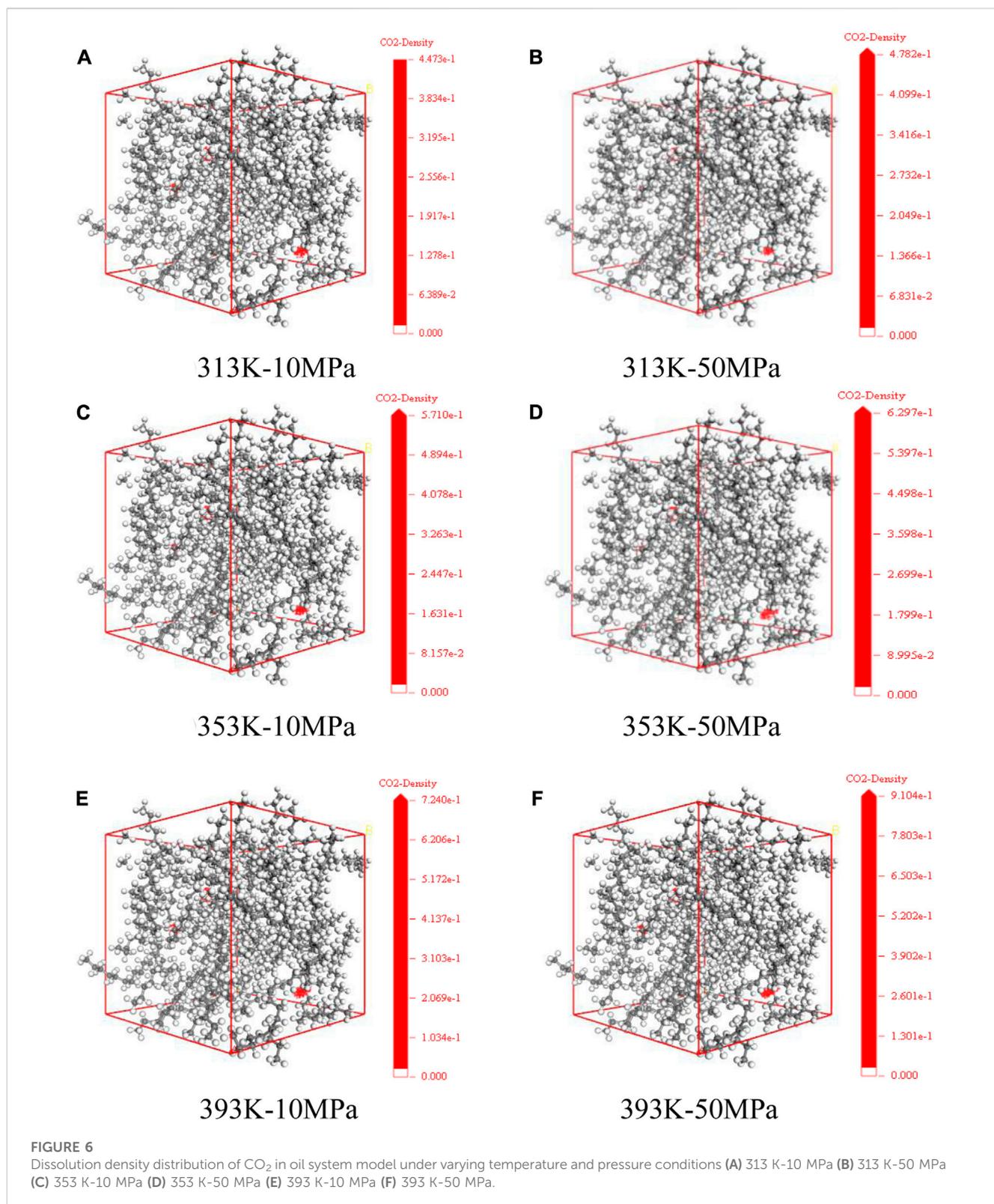
4 Dissolution diffusion coefficient and crude oil mobility

Zhao et al. (2016a) used a PVT instrument to measure the solubility change of CO_2 in crude oil and formation water under reservoir conditions respectively and express those changes through curve representation. It was found that with the enhancement of reservoir pressure, the ability of CO_2 solution in both oil and water enhanced, and the ability of CO_2 solution within oil phase was about 7 times that in water.

TABLE 2 Volume change of oil system at 313 K.

Condition	Pressure MPa	Final model volume Å³	Volume change Å³	Rate of volume change %
Before CO₂ dissolution	10	79690.983	2000.481	2.57
	20	78970.768	1280.266	1.64
	30	78323.617	633.115	0.81
	40	77990.168	299.666	0.39
	50	77817.122	126.620	0.16
After CO₂ dissolution	10	80841.625	3151.123	4.06
	20	80155.734	2465.232	3.17
	30	79452.643	1762.141	2.27
	40	78702.051	1011.549	1.30
	50	78243.050	552.548	0.71

TABLE 3 Volume change of oil system at 353 K.

Condition	Pressure MPa	Final model volume Å³	Volume change Å³	Rate of volume change %
Before CO₂ dissolution	10	82838.956	5148.454	6.63
	20	81842.447	4151.945	5.34
	30	81333.928	3643.426	4.69
	40	80376.023	2685.521	3.46
	50	79339.13	1648.628	2.12
After CO₂ dissolution	10	84905.656	7215.154	9.29
	20	84111.661	6421.159	8.27
	30	83224.991	5534.489	7.12
	40	82042.791	4352.289	5.60
	50	80974.986	3284.484	4.23

TABLE 4 Volume change of oil system at 393 K.

| Condition	Pressure MPa	Final model volume Å³	Volume change Å³	Rate of volume change %
Before CO₂ dissolution	10	87146.066	9455.564	12.17
	20	86125.836	8435.334	10.86
	30	85145.046	7454.544	9.60
	40	83643.014	5952.512	7.66
	50	81906.377	4215.875	5.43
After CO₂ dissolution	10	89014.656	11324.15	14.58
	20	88255.055	10564.55	13.60
	30	86815.055	9125.553	11.75
	40	85815.347	8124.845	10.46
	50	84906.157	7215.655	9.29
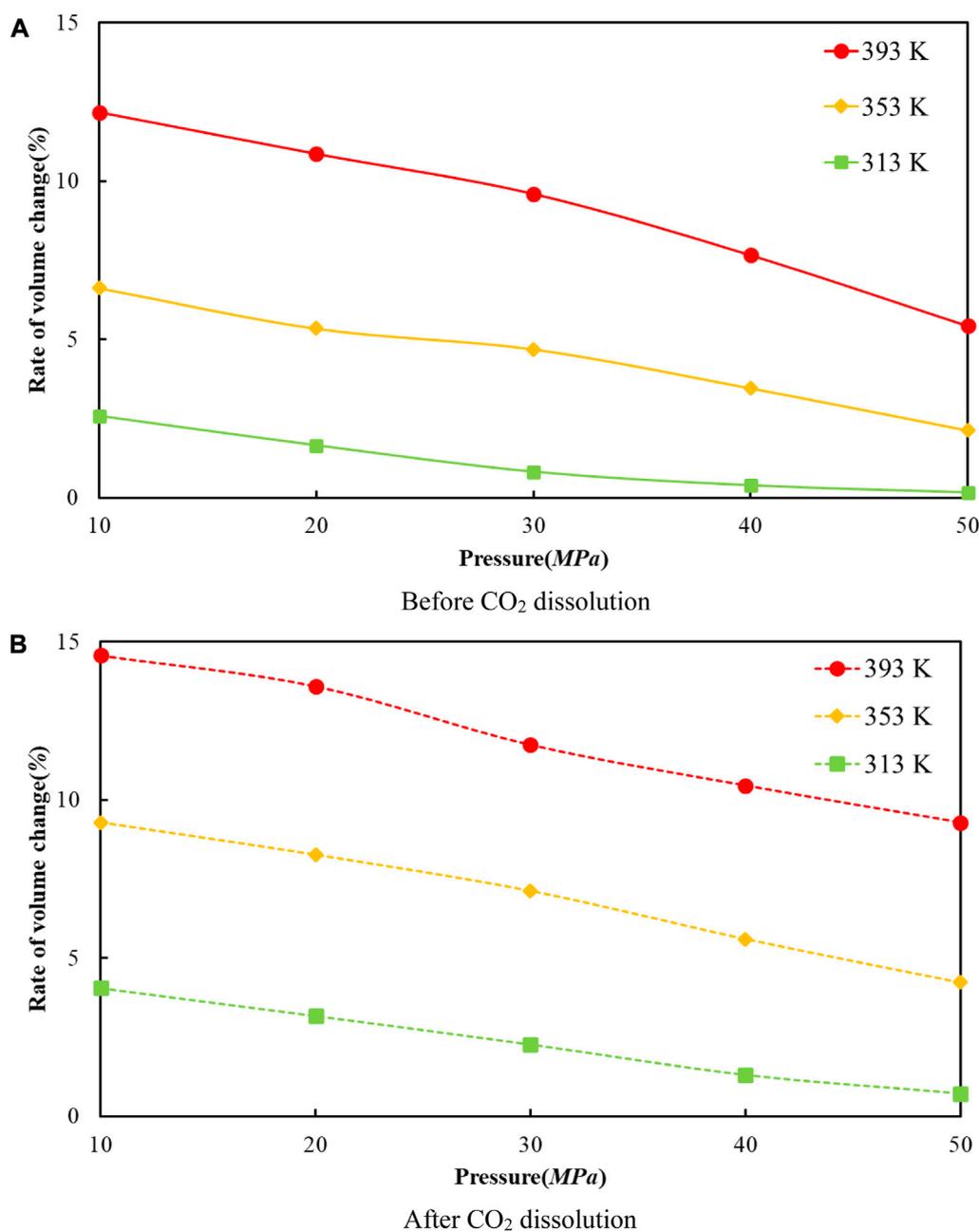
FIGURE 7
The correlation between the volume change rate and pressure of oil system model before and after CO_2 dissolution at different temperatures. **(A)** Before CO_2 dissolution. **(B)** After CO_2 dissolution.
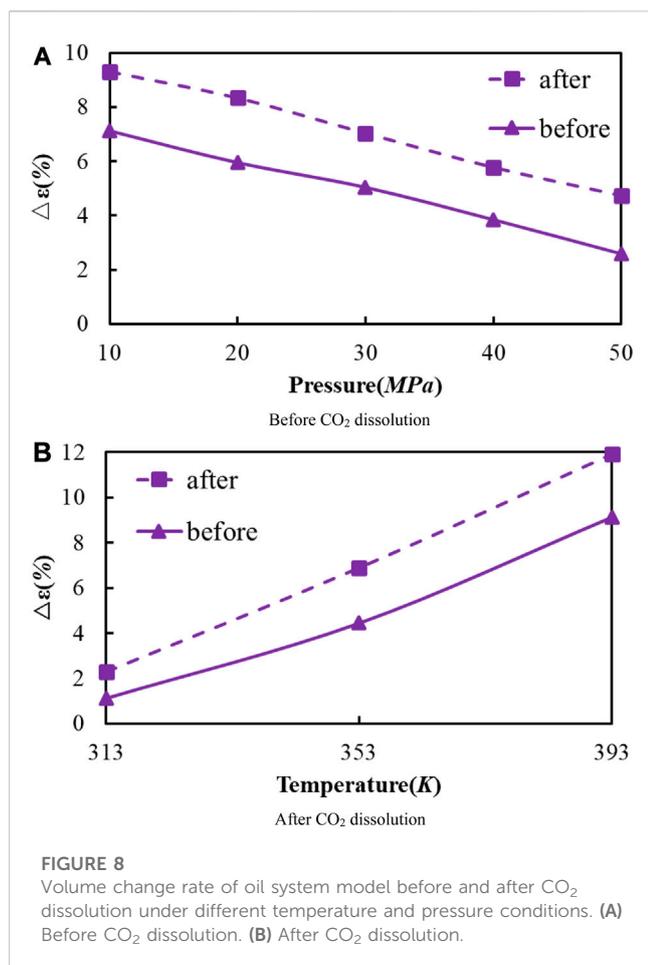
Ao et al. (2019) studied the dissolution and diffusion law in crude oil and brine layer by using the pressure depletion method, and found that the reservoir pressure, temperature and brine concentration all directly affect the dissolution process of CO_2 in brine layer. The higher the salt concentration in the brine layer, the lower the CO_2 dissolution and the slower the diffusion rate.

At a certain temperature, the adsorption isotherm is plotted by calculating the number of small molecules adsorbed in the periodic box at different pressure points, which represents the relationship between the concentration of adsorbed gas and its partial pressure p at a certain temperature. Where the slope of the adsorption isotherm for a pressure value of 0 is the dissolution coefficient S (Jin et al., 2020; Jia et al., 2023):

$$S = \lim_{p \longrightarrow 0} \frac{c}{p} \qquad (4)$$

where S is the dissolution coefficient, dimensionless. This factor represents the maximum number of grams of solute dissolved in 100 g of solution at a given temperature and pressure.

FIGURE 8
Volume change rate of oil system model before and after CO_2 dissolution under different temperature and pressure conditions. **(A)** Before CO_2 dissolution. **(B)** After CO_2 dissolution.

The dissolution coefficient decreases with the increasing temperature. While determining the dissolution rate and final CO_2 dissolution in crude oil is the diffusion coefficient, the larger the diffusion coefficient, the larger the diffusion flux, which determines the gas distribution in the reservoir at different times and affects and improves the physical characteristics of crude oil (Chen et al., 2010). Grogan and Pinczewski (1984) established a mathematical model for the diffusion coefficient under atmospheric pressure conditions by directly observing the interfacial movement of the oil or water phase during CO_2 diffusion. Renner (1988) used artificial cores to test the coefficients of CO_2 and rich gas diffusing motion in crude oil at high pressure. Riazi (1996) used the pressure drop method to study the diffusion coefficients between gas and crude oil (Zhang et al., 2000). Wang (1996) systematically described the CO_2 mixed-phase drive diffusion percolation equation, molecular diffusion coefficient and physical dispersion coefficient models and related experimental determination methods (Li et al., 2001; Fu et al., 2003). Zhao et al. (2016b) proposed an approximate calculation model of the variable diffusion coefficient applicable to the pressure drop method, but the effect of crude oil expansion on diffusion was not considered. In response to the inability of previous authors to comprehensively consider the impacts of varying temperatures and pressures on the diffusion of dissolved CO_2 in crude oil in indoor experiments. This paper takes advantage of

molecular dynamics simulations at the microscopic level to carry out simulation studies.

The diffusion coefficient in this paper is calculated from the mean square displacement and is mainly expressed as (Jin and Chen, 2019; Jin et al., 2020):

$$D = \frac{1}{6N\alpha} \lim_{t \longrightarrow \infty} \frac{d}{dt} \sum_{i=1}^{N\alpha} \left\langle [ri(t) - ri(0)]^2 \right\rangle \tag{5}$$

where Nα denotes the diffusion of atoms in the system and $ri(t)$ represents the displacement vector of molecule i from 0 to time t. The diffusion coefficient is obtained from the best trend line of the MSD curve y = ax + b. It is specifically obtained from the following equation:

$$D = \frac{a}{6} \tag{6}$$

According to the Strokes-Einstein formula, different diffusion coefficients of CO_2 lead to different viscosities of crude oil and ultimately different crude oil fluidity. The two show an inverse relationship, mainly calculated by the following equation:
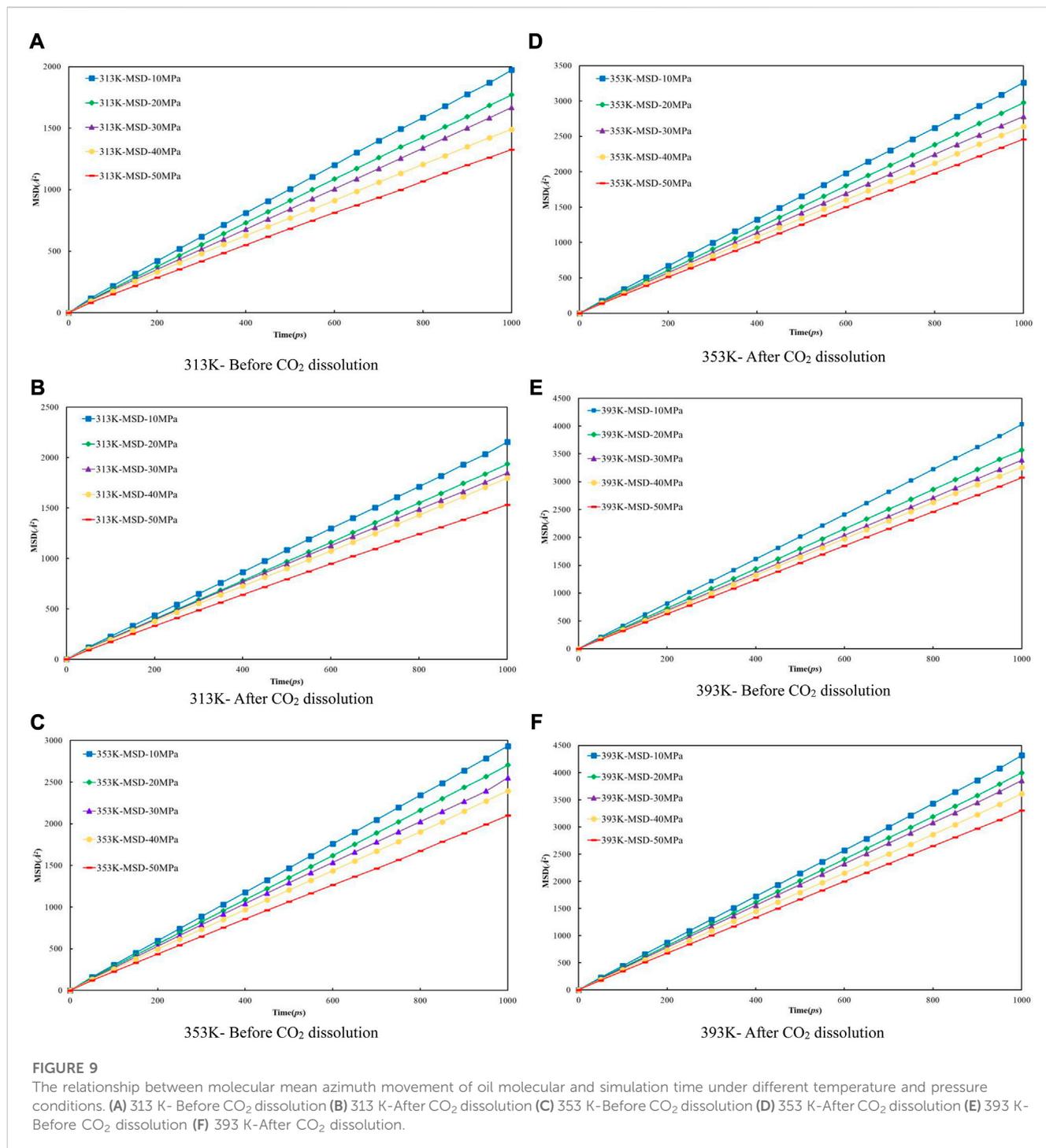
$$\mu = \frac{kT}{6\pi\alpha D} \tag{7}$$

where T represents the simulated temperature, α represents the molecular radius of CO_2, which is approximately 1.65×10^{-8} cm, k denotes the Boltzmann constant, which is 1.38×10^{-23} J/K, D denotes the diffusion coefficient, as well as μ represents the crude oil viscosity.

The dissolution and diffusion coefficients of CO_2 were calculated mainly by Material Studio software. In the simulation process, the software will count the specific dissolution amount of CO_2 at different times, and according to these dissolution amounts, the dissolution coefficient of CO_2 at different times can be calculated. The diffusion coefficient was calculated by calculating the change of Mean Square Displacement of CO_2 over a period of time, and then solving the diffusion coefficient according to linear regression fitting.

5 Results and discussion

5.1 The density distribution of CO_2

Figure 6 shows the distribution state of CO_2 dissolution density in the model of crude oil system that we set up under various temperature and pressure conditions. The red part represents the concentration distribution of CO_2 molecules dissolved in different systems. We count the specific distribution density of CO_2, as shown in the following figure. At the same temperature, with the enhancement of pressure, the dissolving amount of CO_2 within the crude system also increases, and the dissolution density distribution of CO_2 in the crude oil system model enhances. Meanwhile, the ability of CO_2 solubility increases as the temperature rises at the same pressure. This is because of the existence of vast voids among alkane molecules. With the change of external conditions, the movement of CO_2 molecules is intensified, prompting it to enter the voids between alkane molecules.

FIGURE 9
The relationship between molecular mean azimuth movement of oil molecular and simulation time under different temperature and pressure conditions. **(A)** 313 K- Before CO_2 dissolution **(B)** 313 K-After CO_2 dissolution **(C)** 353 K-Before CO_2 dissolution **(D)** 353 K-After CO_2 dissolution **(E)** 393 K-Before CO_2 dissolution **(F)** 393 K-After CO_2 dissolution.

5.2 The expansion law of crude oil model

Since the action of the dissolution of CO_2 into crude oil was done, it promotes the expansion of crude oil. However, the change of external temperature and pressure will make the volume of crude oil model show different variation rules. We calculated the volume of the crude oil model after CO_2 dissolution under different reservoir conditions and found that: the pressure increases, the crude oil system model is compressed and becomes smaller. And the increase of temperature causes the crude oil model to expand further and

become larger in volume. We calculated the system change rate of crude oil system model under different temperature and pressure conditions, as demonstrated in Tables 2, 3, 4 below:

Figure 7 reveals the trends of the volumes of the crude oil system models before and after dissolving CO_2 under varying thermal and pressure conditions. As the pressure increases, the crude oil system model is compressed and the volume of each model decreases. After dissolving CO_2, the volume change rate of the crude oil model reduces linearly, and the volume change rate of each model is comparable to which in the undissolved CO_2 model and smaller

TABLE 5 Diffusion coefficient of oil before and after dissolving CO_2.

Condition	Pressure	Diffusion coefficient	Condition	Pressure	Diffusion coefficient
	MPa	$\times 10^{-4}$ cm^2·s^{-1}		MPa	$\times 10^{-4}$ cm^2·s^{-1}
313 K-Before CO_2 dissolution	10	0.3255	313 K-After CO_2 dissolution	10	0.3559
	20	0.2931		20	0.3203
	30	0.2751		30	0.3050
	40	0.2451		40	0.2954
	50	0.2202		50	0.2533
353 K-Before CO_2 dissolution	10	0.4864	353 K-After CO_2 dissolution	10	0.5415
	20	0.4475		20	0.4942
	30	0.4182		30	0.4632
	40	0.3947		40	0.4385
	50	0.3462		50	0.4081
393 K-Before CO_2 dissolution	10	0.6696	393 K-After CO_2 dissolution	10	0.7137
	20	0.5939		20	0.6620
	30	0.5633		30	0.6385
	40	0.5431		40	0.5956
	50	0.5101		50	0.5485

than that of the undissolved CO_2 model. The interpretation for this phenomenon is that the potential energy difference value from the inner to outer system becomes smaller after CO_2 enters the space between alkane molecules through dissolution and diffusion. At the critical point of dissolution and diffusion, these systems will be in dynamic equilibrium and the influence of external environment becomes weak.

As the temperature increases, the crude oil system model expands and becomes larger in volume. From the simulation results at 313, 353, and 393 K, the average swelling rate of the crude oil model before dissolving CO_2 molecules is 4.01% per 40 K increase.

The average swelling rate after dissolving CO_2 molecules was 4.82% (Figure 8). The increase in temperature promotes the dissolution and diffusion of CO_2 molecules while also prompting the crude oil model to undergo expansion. It is attributed to the enhancement of temperature results in the rise of molecules kinetic energy, the increase of distance between molecules, the increase of space between alkanes, and the extension of the crude oil model system. The enhancement in CO_2 molecules kinetic energy makes it easier to enter into the gaps between alkane molecules, resulting in the increase in dissolution and diffusion ability. As a result, the dissolved amount of CO_2 also increases.

5.3 The prediction of dissolution-diffusion coefficients

Firstly, the density distribution of alkane molecules was calculated, and the distribution of CO_2 density in the models that

we established under various conditions was obtained by simulation to predict the CO_2 dissolving coefficients in the crude oil system and use the coefficients to figure the diffusion coefficient of multi-component crude oil molecules. Figure 9 shows the mean-square displacement (MSD) versus simulation time for the crude oil system model under different pressure conditions. Based on the gradient of the MSD curves, the diffusion coefficients of multicomponent crude oil were calculated as shown in Table 5.

The external pressure has an impact on the volume change rate of the crude oil system model, making it fall off with the pressure increasing, it is due to the decrease of diffusion coefficient before and after the dissolution of CO_2. The diffusion coefficients after dissolving CO_2 are all larger than those before dissolving CO_2, and the diffusion coefficients at all temperature regimes decrease with increasing pressure, among which: the diffusion coefficients for the 313 K regime decrease from 0.3255×10^{-4} cm^2/s at 10 MPa to 0.2202×10^{-4} cm^2/s at 50 MPa and from 0.3559×10^{-4} cm^2/s at 10 MPa to 0.2533×10^{-4} cm^2/s at 50 MPa respectively; the diffusion coefficients of the 353 K system decreased from 0.4864×10^{-4} cm^2/s at 10 MPa to 0.3462×10^{-4} cm^2/s at 50 MPa and from 0.5415×10^{-4} cm^2/s at 10 MPa to 0.4081×10^{-4} cm^2/s at 50 MPa respectively; the diffusion coefficients of the 393 K system decreased from 0.6696×10^{-4} cm^2/s at 10 MPa to 0.5101×10^{-4} cm^2/s at 50 MPa and from 0.7137×10^{-4} cm^2/s at 10 MPa to 0.5485×10^{-4} cm^2/s at 50 MPa respectively.

The molecular kinetic energy and the diffusion coefficient going up while the temperature rises. For example, the diffusion coefficients at 10 MPa pressure increased from 0.3255×10^{-4} cm^2/s at 313 K to 0.6696×10^{-4} cm^2/s at 393 K and from 0.3559×10^{-4} cm^2/s at 313 K to 0.7137×10^{-4} cm^2/s at 393 K

before and after dissolving CO_2, respectively. From these data and analysis in Figure 9, it is able to be indicated that the coefficients of diffusion of the crude oil system after dissolving CO_2 is generally larger than that before dissolution. This is because the dissolved CO_2 occupies the voids of alkane molecules, thus reducing the interaction forces between alkane molecules.

5.4 The influence mechanism of crude oil flow law

The diffusion coefficient of multi-component crude oil before and after dissolving CO_2 is calculated, and the variation of crude oil viscosity can be further calculated according to Eq. 7. The coefficient of diffusion is inversely proportional to the viscosity. The increase of temperature and the dissolution of CO_2 can reduce the viscosity of crude oil and improve the fluidity of crude oil, but the effect of temperature is stronger. Moreover, the increase of temperature accelerates the diffusion of CO_2 molecules into the matrix, which is conducive to the adsorption of CO_2 on the wall and the displacement of crude oil (Lashgari et al., 2019; Chen et al., 2011).

The increase of pressure will increase the intermolecular force of crude oil, inhibit the diffusion, and slightly enhance the crude oil viscosity. However, the enhancement of pressure will promote the dissolution of CO_2, and minish the crude oil viscosity to a certain extent. In general, the increase of pressure will have a weak viscosity reduction effect. Although the increase of pressure will inhibit the diffusion of CO_2 in the crude oil, more CO_2 will enter the reservoir to achieve reservoir acidizing to solve plugging, and also improve permeability and flow capacity (Jia et al., 2021; Gao et al., 2023).

6 Conclusion

In this paper, we established a multi-component model close to the real formation crude oil and employed molecular dynamics simulations to investigate the dissolution and diffusion process of CO_2 in the crude oil systems, and its influence on the mobility of crude oil was examined. By establishing a multi-component crude oil model consistent with the results of experiments, the dissolution-diffusion procedure of CO_2 in multi-component crude oil at 313 K, 353 K, 393 K and 10–50 MPa, in units of 10 MPa were simulated. Our aims were to quantitatively characterize the density distribution of CO_2 dissolved in crude oil, reveal the mechanism of crude oil expansion and improvement of the crude oil mobility due to CO_2 dissolution and diffusion, and systematically analyze the effects of temperature and pressure on the dissolution and diffusion of CO_2. In addition, the research ideas in this manuscript are also applicable to the molecular dynamics simulations of other fluid models. We expect that our study will provide some insights into the mechanism of CO_2-EOR and provide some ideas for molecular dynamics simulations. The following conclusions were obtained:

1) By simulating the reservoir status including temperature and pressure, the dissolving process of CO_2 in multi-component crude oil was observed as well as the density distribution of CO_2 was analyzed; with the change of temperature or pressure, the movement of CO_2 was intensified and driven into the interstices of alkane molecules.

2) The variation of crude oil volume since dissolving CO_2 and the mechanism of varying temperature and pressure on the expansion of crude oil were analyzed. It is concluded that both temperature and pressure promote the action of CO_2 dissolving in petroleum, as well as the crude volume expansion along with temperature enhancing, while compression occurs while the pressure increasing.

3) The coefficient of crude oil diffusion before and after CO_2 dissolution is predicted. The variation trend of diffusing coefficient before and in the back of CO_2 dissolving in crude oil is analyzed, and the impact mechanism of temperature and pressure on diffusing coefficient is clarified.

4) The effects of temperature, pressure as well as CO_2 dissolving on the fluidity of crude oil are studied by combining the variation of diffusion coefficient and SE equation. The increase of temperature and the dissolution of CO_2 can lower the crude oil viscosity and improve the fluid ability of crude oil, but the influence of temperature is stronger. The increase of pressure will have a weak viscosity reduction effect.

Data availability statement

The original contributions presented in the study are included in the article/Supplementary Material, further inquiries can be directed to the corresponding author.

Author contributions

YG: Conceptualization; DW and KL: Investigation; JL: Methodology; LZ: Software; SC: Validation; YK: Writing—original draft; SG: Writing—review and editing. All authors contributed to the article and approved the submitted version.

Acknowledgments

Conflict of interest

Authors YK and LZ were employed by Research Institute of Yanchang Petroleum (Group) Co., Ltd.

The remaining authors declare that the research was conducted in the absence of any commercial or financial relationships that could be construed as a potential conflict of interest.

Publisher's note

References

Ao, W. J., Zhao, R. B., Li, H., Zheng, J. D., Kong, L. P., and Zuo, Q. Q. (2019). Solution-diffusion law of CO2 in crude oil and brine. *Complex Hydrocarb. Reserv.* 12 (3), 51–54. doi:10.16181/j.cnki.fzyqc.2019.03.010

Chen, Y. F., Liao, X. W., Zhao, H. J., and Zhao, X. L. (2010). Determination two key dissolution coefficients in calculation of CO2 storage capacity. *Sci. Technol. Rev.* 28 (01), 98–101. doi:10.1360/972009-1380

Chen, Z. H., Yu, K., and Liu, W. (2011). A preliminary study on the injection-production characteristics and development effects of CO2 miscible flooding: Take the Subei Caoshe oil field as an example. *Eval. Dev. Oil Gas Reserv.* 34 (1), 37–41. doi:10.3969/j.issn.2095-1426.2011.01.007

Fu, G., Du, C. G., Meng, Q. F., and Zhang, G. F. (2003). Diffusion characteristic and loss amount of carbon dioxide gas in FS9 well. *J. Daqing petroleum Inst.* 27 (4), 1–4. doi:10.3969/j.issn.2095-4107.2003.04.001

Gao, H., Wang, C., Cheng, Z. L., Li, T., Dou, L., Zhao, K., et al. (2023). Effect of pressure pulse stimulation on imbibition displacement within a tight sandstone reservoir with local variations in porosity. *Geoenergy Sci. Eng.* 226, 211811. doi:10.1016/j.geoen.2023.211811

Gao, Y. C., Zhao, M. F., Wang, J. B., and Zong, C. (2014). Performance and gas breakthrough during CO2 immiscible flooding in ultra-low permeability reservoirs. *Petroleum Explor. Dev.* 41 (1), 88–95. doi:10.1016/s1876-3804(14)60010-0

Grogan, A. T., and Pinczewski, W. V. (1984). The role of molecular diffusion processes in tertiary CO2 flooding. *Soc. Pet. Eng. AIME, Pap. (United States)* 39 (5), 591–602. doi:10.2118/12706-pa

Guo, M. L., Huang, C. X., Dong, X. G., Zou, Y., and Tang, R. J., (2018). CO2 EOR mechanism of tight sandstone reservoir in Yanchang oilfield. *Chem. Eng. Oil Gas* 47 (2), 75–79. doi:10.3969/j.issn.1007-3426.2018.02.014

Hu, W., Lu, C. Y., Wang, R., Yang, Y., and Wang, X. (2017). Mechanism of CO2 immiscible flooding and distribution of remaining oil in water drive oil reservoir. *Editor. Dep. Petroleum Geol. Recovery Effic.* 24 (5), 99–105. doi:10.13673/j.cnki.cn37-1359/te.2017.05.015

Jia, C. Q., Huang, Z. Q., Sepehrnoori, K., and Yao, J. (2021a). Modification of two-scale continuum model and numerical studies for carbonate matrix acidizing. *J. Petroleum Sci. Eng.* 197, 107972. doi:10.1016/j.petrol.2020.107972

Jia, C. Q., Ren, B., Sepehrnoori, K., Delshad, M., Liu, B., Sun, H., et al. (2023). Numerical studies of hydrogen buoyant flow in storage aquifers. *Fuel* 349, 128755. doi:10.1016/j.fuel.2023.128755

Jia, C. Q., Sepehrnoori, K., Huang, Z. Q., and Yao, J. (2021b). Modeling and analysis of carbonate matrix acidizing using a new two-scale continuum model. *SPE J.* 26 (05), 2570–2599. doi:10.2118/205012-pa

Jia, K. F., Ji, D. C., and Gao, J. D. (2019). The existing state of enhanced oil recovery by CO 2 flooding in low permeability reservoirs. *Unconv. Oil Gas* 6 (1), 107–114.

Jin, Y., and Chen, K. P. (2019). Fundamental equations for primary fluid recovery from porous media. *J. Fluid Mech.* 860, 300–317. doi:10.1017/jfm.2018.874

Jin, Y., Wei, S. M., Chen, K. P., and Xia, Y. (2020). Self-diffusion seepage model. *Acta Pet. Sin.* 41 (6), 737–744.

Ku, H. C., Miao, Y. H., Wang, Y. Z., Chen, X., Zhu, X., Lu, H., et al. (2023). Frontier science and challenges on offshore carbon storage. *Front. Environ. Sci. Eng.* 17 (7), 80. doi:10.1007/s11783-023-1680-6

Lashgari, H. R., Sun, A., Zhang, T. W., Pope, G. A., and Lake, L. W. (2019). Evaluation of carbon dioxide storage and miscible gas EOR in shale oil reservoirs. *Fuel* 241, 1223–1235. doi:10.1016/j.fuel.2018.11.076

Li, C. L. (2018). Gas channeling influencing factors and patterns of CO2-flooding in ultra-low permeability oil reservoir. *Special Oil Gas Reservoirs* 25 (3), 82–86. doi:10.3969/j.issn.1006-6535.2018.03.016

Li, H. Y., Fu, G., and Peng, S. M. (2001). Experimental study on the diffusion coefficients of natural gas. *Petroleum Geol. Exp.* 23 (1), 108–112.

Li, S. L., Tang, Y., and Hou, C. X. (2019). Present situation and development trend of CO2 injection enhanced oil recovery technology. *Reserv. Eval. Dev.* 9 (3), 1–8.

Li, Y., Xiao, K., Huang, C., Wang, J., Gao, M., Hu, A., et al. (2020). Enhanced potassium-ion storage of the 3D carbon superstructure by manipulating the nitrogen-doped species and morphology. *Editor. Dep. Petroleum Geol. Recovery Effic.* 27 (1), 1–10. doi:10.1007/s40820-020-00525-y

Luo, R. H., Hu, Y. L., and Li, B. Z. (2013). Practice of increasing production rate by injecting CO2 into oil and gas fields in China. *Special Oil Gas Reservoirs* 20 (2), 1–7. doi:10.3969/j.issn.1006-6535.2013.02.001

Mi, J. F., and Ma, X. F. (2019). Development trend analysis of carbon capture, utilization and storage technology in China. *Proc. CSEE* 39 (1), 2537–2542. doi:10.13334/j.0258-8013.pcsee.190375

Qin, J. S., Li, Y. L., and Wu, D. B. (2020). CCUS global progress and China's policy suggestions. *Editor. Dep. Petroleum Geol. Recovery Effic.* 27 (1), 20–28. doi:10.13673/j.cnki.cn37-1359/te.2020.01.003

Renner, T. (1988). Measurement and correlation of diffusion coefficients for CO2 and rich-gas applications. *SPE Reserv. Eng.* 3 (2), 517–523. doi:10.2118/15391-pa

Riazi, M. R. (1996). A new method for experimental measurement of diffusion coefficients in reservoir fluids. *J. Petroleum Sci. Eng.* 14 (3/4), 235–250. doi:10.1016/0920-4105(95)00035-6

Shen, P. P., and Liao, X. W. (2009). *The technology of carbon dioxide stored in geological media and enhanced oil recovery.* Beijing: The Press of the Petroleum Industry.

Wang, L. S. (1996). Convective diffusion of driving gases in reservoir fluids(I). *PED* 23 (6), 62–66.

Whorton, L. P., Brownscombe, E. R., and Dyes, A. B. (1952). *Method for producing oil by means of carbon dioxide.* Washington, U.S. Patent No. 2,623,596.

Yuan, S. Y., Wang, Q., Li, J. S., and Han, H. S. (2020). Technology progress and prospects of enhanced oil recovery by gas injection. *Acta Pet. Sin.* 41 (12), 1623. doi:10.7623/syxb202012014

Zhang, Y. J., Zou, Y., Zhang, Y., Wang, L., Liu, D., Sun, J., et al. (2022). Experimental study on characteristics and mechanisms of matrix pressure transmission near the fracture surface during post-fracturing shut-in in tight oil reservoirs. *J. Petroleum Sci. Eng.* 219, 111133. doi:10.1016/j.petrol.2022.111133

Zhang, Y. P., Hyndman, C. L., and Maini, B. B. (2000). Measurement of gas diffusivity in heavy oils. *J. Petroleum Sci. Eng.* 25 (1/2), 37–47. doi:10.1016/s0920-4105(99)00031-5

Zhao, R. B., Ao, W. J., Xiao, A. G., Yan, W., Yu, Z. H., and Xia, X. T. (2016a). Diffusion law and measurement of variable diffusion coefficient of CO2 in oil. *J. China Univ. Petroleum (Ed. Nat. Sci.* 40 (3), 136–142. doi:10.3969/j.issn.1673-5005.2016.03.018

Zhao, S. X., Wang, R., Lv, C. Y., Lun, Z. M., and Zhou, Y. (2016b). Influences of the dissolution on the relative permeability for CO2 flooded low-permeability oil reservoirs. *Petroleum Geol. oilfield Dev. Daqing* 35 (03), 126–129. doi:10.3969/J.ISSN.1000-3754.2016.03.024

Zhao, X. S., Shi, L. H., Wang, W. B., Bai, Y., and Tian, F., (2017). CO2 channeling sealing in ultra-low-permeability reservoirs. *J. Southwest Petroleum Univ. Sci. Technol. Ed.* 39 (6), 131–139. doi:10.11885/j.issn.1674-5086.2016.05.01.61